Multiphoton dissociation of thiophene with 532 and 355 nm

E. Prieto Zamudio, C. Cisneros Gudiño, I. Álvarez Torres, and A. E. Guerrero Tapia

Instituto de Ciencias Físicas, Universidad Nacional Autónoma de México, Cuernavaca, Morelos, México.

Received 6 June 2024; accepted 21 October 2024

The fragmentation of thiophene was investigated using incident laser radiation with two wavelengths, 532 and 355 nm. The results indicate that the intense fragmentation of thiophene molecules decreases at high radiation intensities as was evidenced by the ion C^+. Additionally, the effect of wavelength on the formation of the parent ion, as well as the production of lighter fragments, such as $C_2H_2^+$, is examined. Finally, the dissociation between thiophene and furan to assess the influence of heteroatoms on the fragmentation of these heterocyclic molecules is compared. Our observations reveal the role of hydrogen migration on these heteroatoms.

Keywords: Thiophene; molecular dissociation; multiphotoionization.

DOI: https://doi.org/10.31349/RevMexFis.71.020403

1. Introduction

The study of heterocyclic molecules is important because these compounds play crucial roles in various scientific fields from biology to astrochemistry [1,2]. For instance, the Curiosity Rover found thiophene and some of its derivatives on the surface of Mars [3]. For this reason, is important to understand the role of these compounds when interact with luminous radiation to provide insights into the underlying mechanisms occurring on other planets [4]. In this sense, thiophene (Fig. 1) whose molecular formula is C_4H_4S ($m = 84$ amu) serves as a representative example of heterocyclic molecules [5,6], characterized by an aromatic ring that imparts high stability [7] and symmetry $C_{2\nu}$ [8]. Exploring the fragmentation patterns of thiophene can serve as a valuable starting point for comprehending the behavior of more complex molecules under luminous radiation exposure.

To investigate the dissociation dynamics of thiophene, various fragmentation methods have been employed, including synchrotron radiation [9,10], pyrolysis [11], infrared laser [12], double ionization [13], and theoretical studies too [14]. These diverse approaches highlight the importance of studying small aromatic heterocyclic compounds and are complemented by the mass spectroscopy technique One way to investigate the radiation-matter interaction is to use low energy photons under the multiphoton absorption scheme. In this scenario, molecules require the absorption of more than one photon to reach the ionization energy. For this reason, the intensity and the wavelength of the incident radiation becomes a crucial factor. This method enables the indirect observation of the excited state transitions [15] and can be understood through two mechanisms: ionization-dissociation and dissociation-ionization [16]. This work can shed additional information on the processes involved in the interaction between light radiation and molecules through a multiphoton absorption mechanism. These processes are ubiquitous and occur in diverse environments, from living tissues to interstellar matter [17]. Thiophene can be considered as the analogue molecule of furan, where the oxygen atom is replaced by a sulfur atom. This substitution makes furan less aromatic compared to thiophene because sulfur is less electronegative than oxygen [12]. Consequently, thiophene has greater stability than furan. Based on this fact, the parent ion of furan is expected to undergo more fragmentation than that of thiophene [18]. In a previous article [19] we reported the results obtained for furan. Therefore, in this study we aim to analyze the interaction of thiophene under the same experimental conditions as furan, allowing a direct comparison between these two molecules.

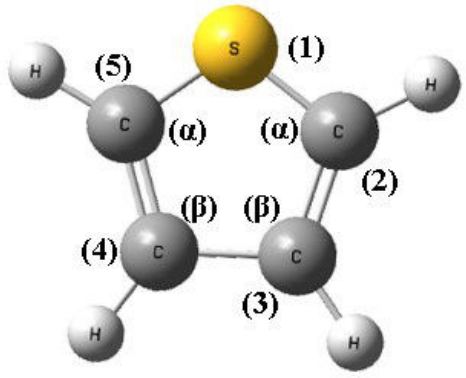

FIGURE 1. Thiophene molecule.

2. Methodology

The experimental setup used in this study was described in a previous work [19]. However, the diagram and the crucial information for this work is presented below (Fig. 2). The sample was obtained from Sigma Aldrich ($>$ 99% purity) and was directly introduced without undergoing any further purification, into a mass spectrometer via a pulsed valve. The pressure before the sample introduction was approximately 10^{-8} mmHg, while the pressure after introduction the sample was around 10^{-6} mmHg. The molecular beam passed through a skimmer before reaching the interaction region,

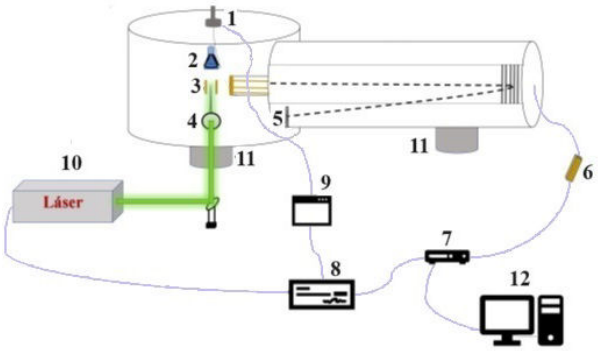

FIGURE 2. Experimental scheme, 1. Pulsed valve, 2. Skimmer, 3. Throttle plates, 4. Focusing lens, 5. Detector, 6. Preamplifier, 7. Multichannel system, 8, Retarder, 9. Valve opening controller, 10 Nd-YAG laser, 11. Molecular turbo pumps, 12. Computer equipment.

where the adiabatic expansion of the sample takes place, significantly reducing the degrees of freedom of the molecules. This step ensures that dissociation or ionization of the thiophene is solely induced by the laser rather than other factors.

The dissociation of thiophene was investigated using a Nd-YAG pulsed laser employment the second (532 nm) and third (355 nm) harmonic, which correspond to the UV-visible range. To examine the effect of radiation intensity on the molecular fragmentation dynamics, a scan of radiation intensities ranging from 2.13×10^9 W/cm^2 to 8.51×10^9 W/cm^2. Positive ions generated during the fragmentation process were accelerated using a potential difference of 1000 V and analyzed using a time-of-flight mass spectrometer coupled with a reflectron. The produced cations were separated based on their mass-to-charge ratio and detected using a multichannel plate detector. The commercial software Origin 9 [20] and Excel were used to analyze the mass spectra obtained. More details on the experimental setup can be found in Ref. [19].

3. Results and discussion

Considering furan as the heteroatom of thiophene, the comparison of its dissociation mechanisms under the same photonic excitation conditions is interesting. Figures 3a) and 3b) show the mass spectra obtained by irradiating furan and thiophene respectively, with wavelengths of 532 nm and 355 nm and at different laser energies. The experiments were carried out within the multiple absorption regime, so the spectra originated from electronic transitions. Even though the ionization energies of furan and thiophene are close (8.88 eV and 8.86 eV respectively) [21], the presence of the heteroatom directly influences the absorption and ionization dynamics at the wavelengths used. So, even though they require the same number of photons to open the dissociative channels, the activation of some of them is different. A very useful element to suggest the ionization channel leading to the observed ion is to know the number of photons involved in the absorption. The slope of the linear part of the relationship between the logarithms of the ionic current and laser intensity is proportional to the number of photons needed to achieve the ionization state [22]. This is calculated according to the Eq. (1)

$$Y = \sigma_n I_n, \tag{1}$$

where Y is the ionic current, n the process order and σ_n the nth order cross section [22]. Although n is generally not an integer since its value also depends on other internal processes, the order is considered as the minimum number of photons necessary to reach the state of ionization or dissociation [22,23]. The next Table I shows the photons calculated at wavelength of 355 nm according to Eq. (1) for the formation of some of the observed fragments.

TABLE I.

Mass (uma)	Fragment	Absorbed photons
1	H^+	3.8
12	C^+	1.8
13	CH^+	3.8
24	C_2^+	2.9
32	S_2^+	3.1
39	$C_3H_3^+$	2.3
44	CS^+	2.6
45	CSH^+	2.1

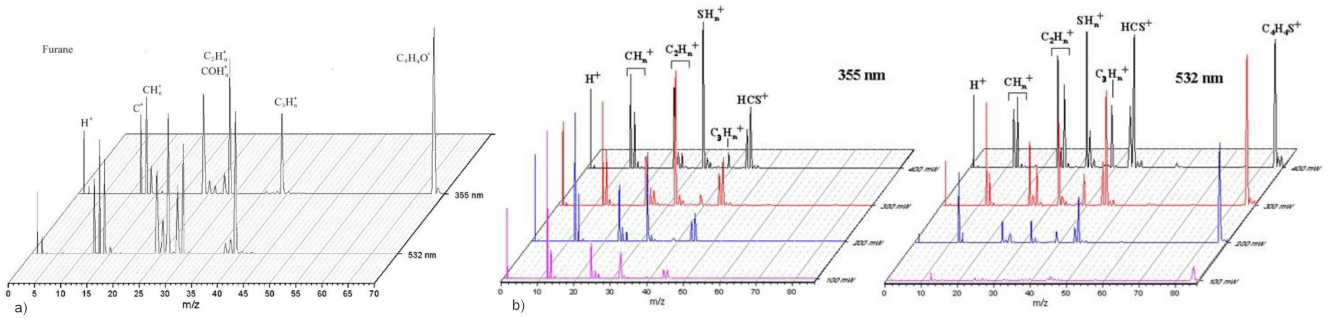

FIGURE 3. a) Mass spectra of Furane obtained by multiphoton ionization with $\lambda = 355$ nm and $\lambda = 532$ nm. Radiation intensity is 7.66×10^{-9} W/cm^2 [19]. b) Mass spectra of thiophene obtained by multiphoton ionization with $\lambda = 355$ nm and $\lambda = 532$ nm. Radiation intensity in the range of 2.13×10^9 W/cm^2 to 8.51×10^9 W/cm^2.

VUV photoabsorption studies [6,24] indicate a strong absorption band for thiophene in the range of 6.55 eV to 7.70 eV, with the highest absorption intensity corresponding to the $\pi \rightarrow \pi^*$ transitions [25]. This transition is achieved by absorbing two 355 nm and three 532 nm photons. With any of the wavelengths and once the molecule is excited, in principle the absorption of an additional photon would be enough to achieve ionization of the parent ion.However, it is observed in the spectra that this $C_4H_4S^+$ ion only appears with 532 nm radiation. The response to this behavior is found in the different excited states that are reached with the absorption of one or another of the incident photons. The observation of the parent molecular ion in furan at 355 nm and in thiophene at 532 nm, even though they have close ionization energies, is attributed to resonance effects in which the absorption of the photons coincides with an excited eigenstate facilitating direct ionization and the consequent presence of the parent molecular ion. The similarity in the fragmentation patterns indicates that the dissociation-ionization and ionization-dissociation processes lead to comparable fragmentation results regardless of which process occurs first.

According to Fig. 3b), the H^+ ion presents an almost constant behavior at 355 nm, but at 532 nm, the intensity increases as the incident radiation energy increases. The origin of the H^+ can be considered as result of the deprotonation of thiophene, mainly of those H in the alpha position. This preference lies in the greater stability of the C_4H_3S alpha isomer compared to the position of the corresponding beta isomer [26]. The energy required to eliminate alpha H is approximately 4.99 eV [26], therefore the absorption of two photons of any wavelength is required. Rennie *et al.* [18] using radiation synchrotron propose as the main fragmentation mechanisms of thiophene those summarized in the following Table II

It is observed in Fig. 3b) that the signal corresponding to mass 39 ($C_3H_3^+$) in Table II is small at 355 nm and a little larger at 532 nm, growing as the radiation intensity increases. More notable is mass 45 (CHS^+) that appears with both incident wavelengths. The signal associated with mass 58 $C_2H_2S^+$) is barely outlined as the intensity of the incident radiation of both wavelengths increases, and those proposed in Table II with masses 69 and 83 are not recorded in Fig. 3b). The absence of signals from some of the fragments is explained by the differences in the energy of the incident photons in each of the experiments. Between 2-4 eV in the present case, and between 12-28 eV of synchrotron radiation in the other case.

TABLE II.

$C_4H_4S^{+\bullet} \rightarrow C_3H_3^+$ $(m/q = 39)$ + $CHS^\bullet$
$C_4H_4S^{+\bullet} \rightarrow CHS^+$ $(m/q = 45)$ + $C_3H_3^\bullet$
$C_4H_4S^{+\bullet} \rightarrow C_2H_2S^{+\bullet}(m/q = 58)$ + C_2H_2
$C_4H_4S^{+\bullet} \rightarrow C_3HS^+$ $(m/q = 69)$ + $CH_3^\bullet$
$C_4H_4S^{+\bullet} \rightarrow C_4H_3S^+$ $(m/q = 83)$ + $H^\bullet$

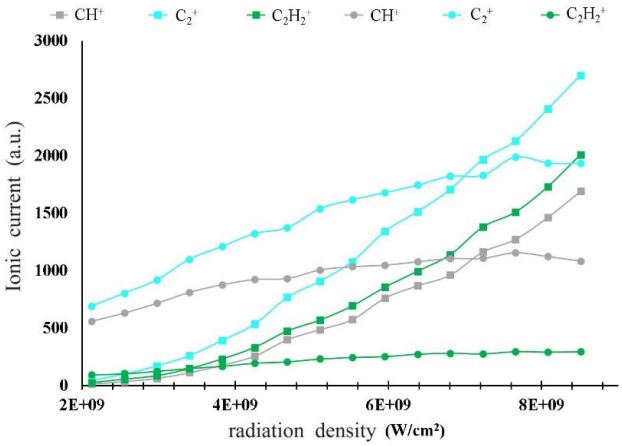

FIGURE 4. Comparison of the ionic current of the ions CH^+, C_2^+, $C_2H_2^+$ obtained with $\lambda = 355$ nm (•) and $\lambda = 532$ nm (□) in the range of 2.13×10^9 to 8.51×10^9 W/cm^2

The CH^+ ion could be considered the main precursor of the C^+ ion, however, according to what was observed in the ionic currents (Fig. 4), the behavior of these ions is contrary to those expectations. One possible channel is the one that considers the breaking of the C-C bond of acetylene. It is expected that by increasing the photon density, larger fragmentation channels will be activated, leading to the production of ions of lower mass, such as C^+.

The weak CH_2^+ signal, at both wavelengths, indicates the migration of H_α during the fragmentation process. This requires less energy compared to H_β atoms [27].

The absence of the parent ion at 355 nm and the appearance of the $C_nH_n^+$ and SH_n fragments suggest strong fragmentation of the parent ion at this wavelength. It could be considered that this fragmentation originates from the Coulomb explosion, however this mechanism would lead to the generation of fragments with multiple charges [28], a situation that is not observed in the spectra. Being in the multiple absorption regime, four photons of 532 nm (9.28 eV) or three of 355 nm (10.47 eV) are required to achieve a first ionization of the original fragment. This is 0.43 eV and 1.6 eV respectively higher than the energy needed to extract the first electron from thiophene (8.86 eV) [21]. As the density of photons increases, its probability of absorbing more of them increases and the opening of more dissociation channels is achieved, undergoing complete fragmentation [29] and reaching lower mass fragments such as C^+ and H^+.

The $C_2H_2^+$ ion is important since it has been reported as a neutral fragment in the production of C_2H_2+$CH_2CS^{\bullet+}$ [18]. Theoretical studies [25] suggest that the formation of this fragment comes from the breaking of the double bonds between the C-S and the C-C. Furthermore, its presence is favored for $\lambda = 532$ nm, which shows the strong dependence of its production on the wavelength. As can be seen in the spectra [Fig. 3b)], most of the ions generated are the same at both wavelengths, although at different intensities.

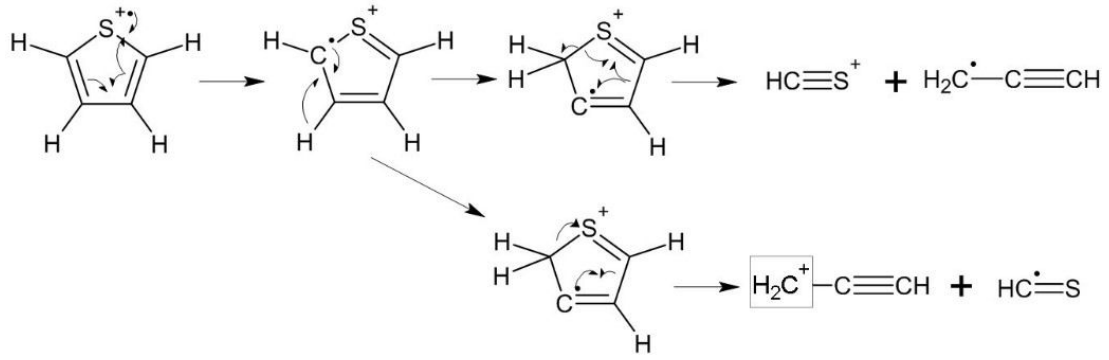

FIGURE 5. Proposed fragmentation mechanism to produce HCS^+ and $C_3H_3^+$ ions from $C_4\ H_4S^+$.

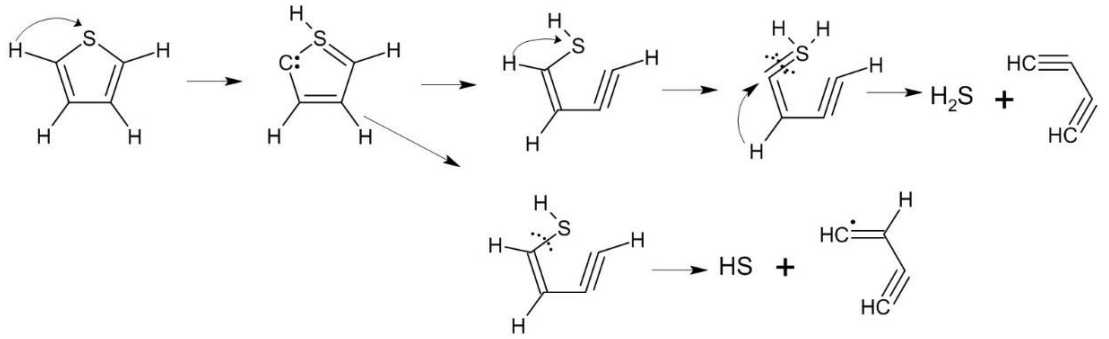

FIGURE 6. Proposed fragmentation mechanism to produce SH_2^+ and SH^+ ions.

The $C_3H_3^+$ and HCS^+ ions (similar equivalents to $C_3H_3^+$ and HCO^+ in furan) were identified at both wavelengths. The production of these ions is expected to come from similar fragmentation mechanisms. The signal intensity of these ions was strongest at the wavelength $\lambda = 532$ nm, where the parent ion appears. The difference in peak heights between HCS^+ and $C_3H_3^+$ could be attributed to the difference in the activation energies required for their formation, which are 6.9 eV and 6.5 eV respectively [30]. Although $C_3H_3^+$ requires less energy, three-photon absorption with a wavelength of $\lambda = 532$ nm (6.96 eV) is closer to the activation energy of HCS^+. Figure 5 shows the possible mechanisms to produce these fragments from the parent ion and Table III their activation energy [30,32].

In the case of $C_2H_2S^+$, although it requires little energy for its formation, it does not appear at 355 nm and a very weak signal is barely perceived at 532 nm. This may be related to the presence of the $C_2H_2^+$ ion, suggesting that they come from competitive mechanisms.

TABLE III.

Ion	Activation Energy (eV)
$C_2H_2S^+$	4.6 ± 0.7
CHS^+	6.9 ± 0.7
$C_3H_3^+$	6.5 ± 0.7

The production of the SH^+ and SH_2^+ fragments involve the migration of one and two hydrogens respectively. In the first case, a migration of H_α to S takes place, subsequently the first breakage of the ring takes place, creating the possibility of a second breakage for the release of the SH^+ ion. For (SH_2) after the migration of H_β to S, a second migration of H_β to C_α takes place accompanied by a C-S cleavage. Subsequently, the second migration of H_α to S takes place and finally the second C-S bond is broken where SH_2 is produced [31] (Fig. 6).

It can be seen in the mass [Figs. 3a), 3b)] and current (Fig.4) spectra that the intensity of some ions at low powers of incident radiation is greater with $\lambda = 355$ nm. This is not surprising since the higher photon energy at this wavelength activates the ionization and dissociation channels with a lower number of absorbed photons. For higher energy densities, the multiple absorption at $\lambda = 532$ nm also activates these dissociative channels, reversing the trend and obtaining higher intensities of the fragments.

In particular, the HCS^+ and $C_3H_3^+$ fragments are more abundant for $\lambda = 532$ nm, which suggests a possible association with the parent ion in a direct dissociation process $C_4H_4S^+$ to $C_3H_3^+$ + HCS or $C_3H_3^+$ HCS^+. The CS^+ ion is recorded together with the HCS^+ so it can be interpreted that its formation is derived from the latter through the loss of a hydrogen. The ionic fragments S^+ and HCS^+ appear with great intensity for both wavelengths [see Fig. 7a), b)]. The large sulfur signal is very important since thiophene is one of

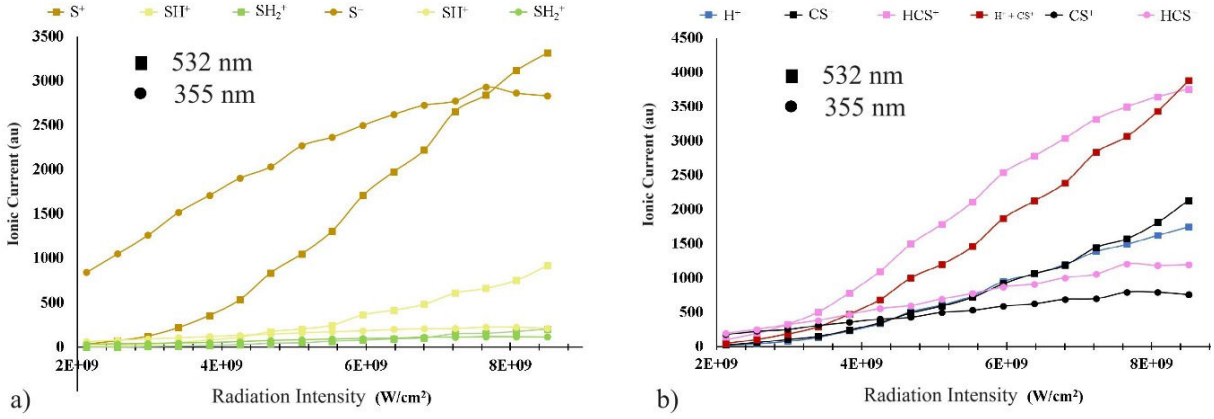

FIGURE 7. SH_n^+ and H_n CS^+ fragments at $lambda = 532$ nm and $lambda$ nm. Power density at $2 - 8 \times 10^9$ W/cm^2.

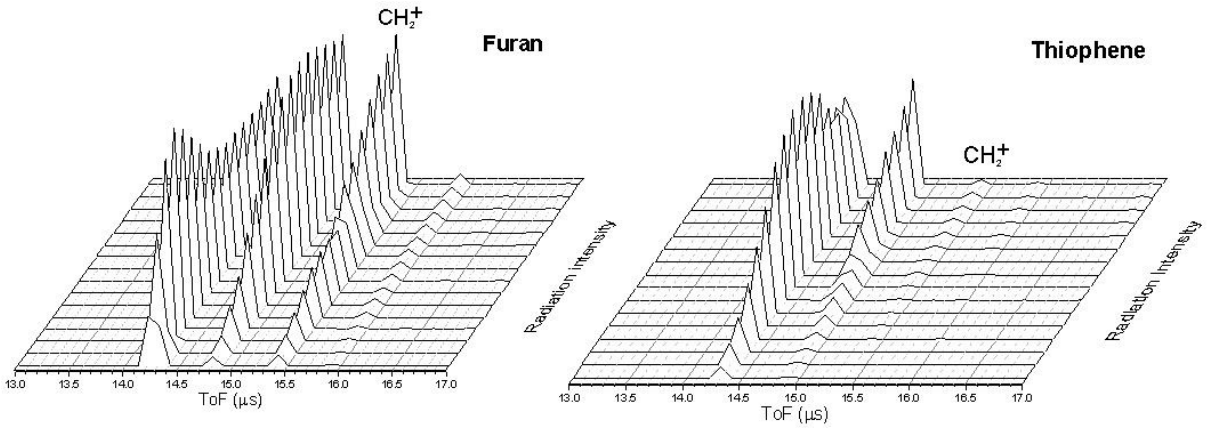

FIGURE 8. Ionic Current behavior of CH_2^+ in furan and thiophene with $lambda = 532$ nm.

the most complicated compounds to desulfurize [33,35], consuming a large amount of hydrogen during the industrial hydrodesulfurization process [33,34,35]. S^+ is formed from the migration of the hydrogen atom predominantly from the alpha positions [33] followed by the cleavage of the C-S bond. Within this process, the cleavage of the C-S bond is crucial since it initiates the fragmentation of thiophene and is the factor that improves desulfurization [35,36]. According to Fig. 7, the desulfurization of thiophene is higher with 355 nm in almost the entire range of incident radiation used. In contrast, the migration of a hydrogen towards sulfur increases with $\lambda = 532$ nm.

The above agrees with the fact that photons with $\lambda = 355$ nm are more energetic and therefore the energy necessary to start this process is achieved with lower radiation intensity. On the other hand, it is observed that the HCS^+ and CS^+ ions as well as the parent ion are produced in greater quantities for $\lambda = 532$ nm. Likewise, the trend of the CS^+ ion is like that shown by the H^+ fragment during almost the entire radiation interval. Consequently, it is possible that the CS^+ ion originates from the deprotonation of the HCS^+ ion as shown in the following reactions (2) and (3).

$$HCS^+ \rightarrow CS^+ + H, \tag{2}$$

$$HCS^+ \rightarrow CS + H^+. \tag{3}$$

One explanation for the similarity of the ionic current (IC) of the CS^+ and H^+ ions is that they come from a competitive dissociation mechanism between reactions Eqs. (2) and (3). Consequently, it is expected that the sum of IC of these ions should exceed that of the HCS^+ ion, which can be verified in Fig. 7. In support of the above, Fig. 7 shows how IC of HCS^+ decreases while that corresponding to CS^+ increases.

On the other hand, another significant effect associated with the heteroatom is the migration of hydrogen that gives rise to the CH_2^+ ion. Effect that appears in both furan and thiophene (Fig. 8). In the case of furan, it presents an accelerated growth of intensity with $\lambda = 532$ nm at low powers of incident radiation, but the same does not occur with thiophene, where it is barely perceptible at these powers (Fig. 8). This difference in CH_2^+ formation between furan and thiophene highlights the importance of considering heteroatoms in the activation of ionization and dissociation mechanisms.

4. Conclusions

- The presence of low molecular weight S^+, C^+ and H^+ fragments at $\lambda = 355$ nm can be considered to come from the complete fragmentation of thiophene.
- In the case of S^+ it indicates that the heteroatom tends to retain the charge during dissociation.
- The relationship in the growth of H^+, C^+ and HC^+ ions with the photon density at $\lambda = 532$ nm, points to CH^+ as the precursor of these ions.
- The differences in the production of the fragments obtained from the dissociation of furan and thiophene highlight the effect of the heteroatom.
- The excited state of the molecule that is reached when irradiating with $\lambda = 355$ nm or with $\lambda = 532$ nm determines the absence or appearance, respectively, of the original $C_4H_4S^+$ ion. Different ionization methods lead to the products $C_3H_3^+$ and HCX^+ (with X= oxygen or sulfur).
- Coulomb explosion is ruled out for complete fragmentation of the parent ion due to the absence of multiply charged ions.

Declaration of interest

The authors declare that they have no known competing financial interests or personal relationships that could have appeared to influence the work reported in this paper

Funding

This work was supported by UNAM-DGAPA PAPIIT IN104423

1. A. Alizadeh and R. Rezaiyehraad, Recyclization of 3-formylchromone with phenacyl thiocyanate: fast and efficient access to thiophenes and 2-aminothiophenes bearing oacylphenol moiety. *J. Sulphur Chem.* **43** (2022) 264, https://doi.org/10.1080/17415993.2021.2007920
2. F. S. Mehdhar, E. Abdel-Galil, A. Saeed, E. Abdel-Latif, and G. E. Abd el-Ghani, Synthesis of new substituted thiophene derivatives and evaluating their antibacterial and antioxidant activities. *Polycycl Aromat Compd*, **43** (2022) 4496, https://doi.org/10.1080/10406638.2022.2092518
3. Heinz and D. Schulze-Makuch. Thiophenes on Mars: Biotic or Abiotic Origin? *Astrobiology*, **20** (2020) 552, https://doi.org/10.1089/ast.2019.2139
4. S. Falcinelli *et al*., Kinetic energy release in molecular dications fragmentation after VUV and EUV ionization and escape from planetary atmospheres. *Planetary Space Science*, **99** (2014) 149, http://dx.doi.org/10.1016/j.pss.2014.04.020.
5. M.N. Kawade, D. Srinivas, H.P. Upadhyaya. Kinetics of gas phase OH radical reaction with thiophene in the 272-353 K temperature range: A laser induced fluorescence study. *Chem. Phys. Lett.* **682** (2017) 154, http://dx.doi.org/10.1016/j.cplett.2017.05.072.
6. M.H. Palmer, I.C. Walker and M. F. Guest. The electronic states of thiophene studied by optical (VUV) absorption, near-threshold electron energy-loss (EEL) spectroscopy and ab initio multi-reference configuration interaction calculations. *Chem. Phys.* **241** (1999) 275, https://doi.org/10.1016/S0301-0104(98)00425-X.
7. Z. Yan, Y. Luo, B. Chen, F. Wang, L. Chen, Z. Wang, P. Zhao, J. Kang, Z. Fu, Y. Jin, Y. Wang and C. Xia. Thiophene-based conjugated ultra-micropore rigid polymers for selective xenon capture. *Chem. Eng. J.* **453** (2023) 139934, https://doi.org/10.1016/j.cej.2022.139934.
8. D.M.P. Holland, L. Karlsson and W. Von Niessen. The identification of the outer valence shell p-photoelectron bands in furan, pyrrole and thiophene. *J. Electron. Spectrosc. Relat. Phenom.* **113** (2001) 221, https://doi.org/10.1016/S0368-2048(00)00427-8
9. R. G. Hayes and W. Eberhardt. Electron-ion coincidences studies of the fragmentation of thiophene and of tetrahydrothiophene upon core ionization. *J. Chem. Phys.* **94** (1991) 397, https://doi.org/10.1063/1.460730.
10. M.S.P. Mundim, A. Mocellin, N. Makiuchi, A. Naves de Brito, M. Attie and N. Correia. Study of thiophene inner shell photofragmentation. *J. Electron Spectrosc. Relat. Phenom.* **155** (2007) 58, https://doi.org/10.1016/j.elspec.2006.12.018
11. J.K. Winkler, W. Karow and P. Rademacher. Gas-phase pyrolysis of heterocyclic compounds, part 1 and 2: flow pyrolysis and annulation reactions of some sulfur heterocycles: thiophene, benzo[b]thiophene, and dibenzothiophene. A product-oriented study. *J. Ana.l Appl. Pyrolysis.* **306** (2004) 295, https://doi.org/10.1016/S0165-2370(00)00218-7.
12. A. K. Nayak, S. K. Sarkar, R. S. Karve, V. Parthasarathy, K.V.S. Rama-Rao, J.P. Mittal, S.L.N.G. Krishnamachari and T. V. Venkitachalam. Infrared Laser Multiple Photon Dissociation of Thiophene in Gas Phase. *Appl. Phys. B.* **48** (1989) 437, https://doi.org/10.1007/BF00694545
13. P. Linusson, L. Storchi, F. HeijkenskjÃ¶ld, E. Andersson, M. Elshakre, B. Pfeifer, M. Colombet, J. H. D. Eland, L. Karlsson, J. E. Rubensson F. Tarantelli and R. Feife. Double photoionization of thiophene and bromine-substituted thiophenes. *J. Chem. Phys.* **129** (2008) 234303, https://doi.org/10.1063/1.3039082.
14. E.G. Naz and M. Paranjothy. Theoretical studies of unimolecular decomposition of thiophene at high temperatures. *Electron. Struct.* **3** (2021) 045003, https://doi.org/10.1088/2516-1075/ac391f.

15. B. Barc, M. Ryszka, J. Spurrell, M. Dampc, P. Limao-Vieira, R. Parajuli, N.J. Mason and S. Eden. Multi-photon ionization and fragmentation of uracil: Neutral excited-state ring opening and hydration effects. *J. Chem. Phys.* **139** (2013) 244311, https://doi.org/10.1063/1.4851476.

16. A. Gedanken, M. B. Robin and N.A. Kuebler. Nonlinear photochemistry in organic, inorganic, and organometallic systems. *J. Chem.* **86** (1982) 4096, https://doi.org/10.1021/j100218a004.

17. E. Kukk *et al.*, Internal energy dependence in x-ray-induced molecular fragmentation: An experimental and theoretical study of thiophene. *Phys. Rev. A.* **91** (2015) 043417, https://doi.org/10.1103/PhysRevA.91.043417.

18. E.E. Rennie, D.M.P. Holland, D.A. Shaw, C.A.F. Johnson and J.E. Parker, A study of the valence shell spectroscopic and thermodynamic properties of thiophene by photoabsorption and photoion spectroscopy. *Chem. Phys*. **62** (2002) 123, https://doi.org/10.1016/j.chemphys.2004.07.029.

19. E. Prieto, C. Cisneros, L.X. Hallado, I. Álvarez and A.E. Guerrero. Effect of radiation intensity on the fragmentation of furan through multiphoton ionization at 532 and 355 nm. *Radiat. Phys. Chem.* **198** (2002) 110261, https://doi.org/10.1016/j.radphyschem.2022.110261.

20. Origin(Pro), Version Number (Version 2019). OriginLab Corporation, Northampton, MA, USA.

21. P. J. Linstrom *et al*., NIST Chemistry WebBook, NIST Standard Reference Database Number 69, National Institute of Standards and Technology, Gaithersburg MD, 20899, https://doi.org/10.18434/T4D303

22. M.J. DeWitt and R.J. Levis, Concerning the ionization of large polyatomic molecules with intense ultrafast lasers. *J. Chem. Phys.* **110** (1999) 11368, https://doi.org/10.1063/1.479077

23. J.C. Poveda, Doctoral Thesis. Fotoionización y Fotodisociación de Hidrocarburos Aromáticos Policíclicos. National University Autonomous of México, pp. 29, (2009).

24. J. Wan, M. Hada, M. Ehara and H. Nakatsuji, Electronic excitation spectrum of thiophene studied by symmetry adapted cluster conguration interaction method. *Chem. Phys.* **114** (2001) 842, https://doi.org/10.1063/1.1332118

25. S. Salzmann, M. Kleinschmidt, J. Tatchen, R. Weinkauf and C. M. Marian. Excited states of thiophene: ring opening as deactivation mechanism. *Phys. Chem. Chem. Phys.* **10** (2008) 380, https://doi.org/10.1039/B710380H

26. L.M. Culberson and A. Sanov, Electronic states of thiophenyl and furanyl radicals and dissociation energy of thiophene via photoelectron imaging of negative ions. *J. Chem. Phys*. **134** (2011) 204306, https://doi:10.1063/1.3593275.

27. E.E. Rennie, L. Cooper, L.G. Shpinkova, D.M.P. Holland, D.A. Shaw and P.M. Mayer. Threshold photoelectron photoion coincidence spectroscopy sheds light on the dissociation of pyrrole and thiophene molecular ions. *Int. J. Mass Spectrom.* **290** (2010) 142, https://doi:10.1016/j.ijms.2009.12.002

28. P. Tzallas *et al.*, Coulomb explosion in aromatic molecules and their deuterated derivatives. *J. Photochem. Photobiol. C.* **332** (2018) 236, https://doi.org/10.1016/S0009-2614(00)01285-9.

29. H.P. Upadhyaya, Ground-state dissociation pathways for the molecular cation of 2-chlorothiophene: A time-of-flight mass spectrometry and computational study. *RCM* **33** (2019) 1598, https://doi.org/10.1002/rcm.8497

30. H. Lim, D.G. Schultz, E.A. Gislason and L. Hanley. Activation energies for the fragmentation of thiophene ions by surface induced dissociation. *J. Phys. Chem. B.* **102** (1998) 4573, https://doi.org/10.1021/jp980342f

31. Li-Xia Ling, Ri-Guang Zhang, Bao-Jun Wang, Ke-Chang Xie. Density functional theory study on the pyrolysis mechanism of thiophene in coal. *J. Mol. Struct. THEOCHEM*. **905** (2009) 8, https://doi.org/10.1016/j.theochem.2009.02.040

32. Xinli Song and C.A. Parish Pyrolysis Mechanisms of Thiophene and Methylthiophene in Asphaltenes., *J. Phys. Chem. A.* **115** (2011) 2882, https://doi.org/10.1021/jp1118458.

33. R.D. Adams, O Sung Kwon and J.L. Perrin. The effect of a vinyl substituent on the ring opening of a substituted tetrahydrothiophene at a triosmium center. *Chem*. **584** (1999) 223, https://doi.org/10.1016/S0022-328X(99)00143-6

34. S. Meng, W. Li, Z. Li and H. Song, Non-thermal plasma assisted catalytic thiophene removal from fuel under different atmospheres. *J. Clean. Prod*. **369** (2022) 133282, https://doi.org/10.1016/j.jclepro.2022.133282.

35. N.Y. Dzade and N.H. de Leeuw. Adsorption and desulfurization mechanism of thiophene on layered FeS(001), (011), and (111) surfaces: A dispersion-corrected Density Functional Theory study. *J. Phys. Chem. C*. **122** (2018) 359, https://doi.org/10.1021/acs.jpcc.7b08711,2018.

36. J.F. Lang and R.I. Masel, The adsorption of thiophene and tetrahydrothiophene on several faces of platinum. *Surf. Sci.* **183** (1987) 44, https://doi.org/10.1016/S0039-6028(87)80335-7